Advances in Computational Design, *Vol. 6, No. 1 (2021) 31-42*
DOI: https://doi.org/10.12989/acd.2021.6.1.31

Optimal fin planting of splayed multiple cross-sectional pin fin heat sinks using a strength pareto evolutionary algorithm 2

Sanchai Ramphueiphad* and Sujin Bureerat

Sustainable and Infrastructure Research and Development Center, Department of Mechanical Engineering, Faculty of Engineering, Khon Kaen University, Khon Kaen, Thailand

(Received November 14, 2019, Revised July 8, 2020, Accepted October 28, 2020)

Abstract. This research aims to demonstrate the optimal geometrical design of splayed multiple cross-sectional pin fin heat sinks (SMCSPFHS), which are a type of side-inlet-side-outlet heat sink (SISOHS). The optimiser strength Pareto evolutionary algorithm 2 (SPEA2) is employed to explore a set of Pareto optimal solutions. Objective functions are the fan pumping power and junction temperature. Function evaluations can be accomplished using computational fluid dynamics (CFD) analysis. Design variables include pin cross-sectional areas, the number of fins, fin pitch, thickness of heat sink base, inlet air speed, fin heights, and fin orientations with respect to the base. Design constraints are defined in such a way as to make a heat sink usable and easy to manufacture. The optimum results obtained from SPEA2 are compared with the straight pin fin design results obtained from hybrid population-based incremental learning and differential evolution (PBIL-DE), SPEA2, and an unrestricted population size evolutionary multiobjective optimisation algorithm (UPSEMOA). The results indicate that the splayed pin-fin design using SPEA2 is superior to those reported in the literature.

Keywords: air-cooling heat sink; computational fluid dynamic simulation; strength Pareto evolutionary algorithm; multi-objective optimisation; evolutionary computation

1. Introduction

An air-cooled heat sink is the most commonly used device for removing heat from electronic equipment due to its major advantages of being simple to form, low cost and highly reliable. It works by utilizing forced convection of heat from heat sink fins which are transferred from the heat sink base attached to an electronic device (Kanyakam and Bureerat 2011, Srisomporn and Bureerat 2008). Air-cooling heat dispersion with various types of fins has received significant attention for some decades, while many design techniques have also been proposed.

Using nanofluid for the cooling of electronic equipment has been investigated (Bahiraei 2019, Bahiraei 2018, Bahiraei and Heshmatian 2017). In past research (Yang *et al.* 2019). Minimization of construction operation costs for cylindrical pin fin heat sinks in-line was investigated. The results show that when single degree of freedom optimisation is performed, the minimum operating cost and the optimum construction cost are different under different values of fin-

*Corresponding author, Ph.D., E-mail: sanchai.ra@rmuti.ac.th

http://www.techno-press.org/?journal=acd&subpage=7 ISSN: 2383-8477 (Print), 2466-0523 (Online)

material fraction (FMF), heat transfer load (HTL), fluid velocity (FV), and the cost ratio is in the parameter research range; when double degree of freedom optimisation is performed, the operating cost of the pin-fin heat sinks (PFHS) increases as the height-to-width aspect ratio of the PFHS increases. Analytical 3D modelling of the plate fin heat sink for forced convection was used in an optimisation routine to reduce the weight of a current heat sink to demonstrate that analytical models can quickly and accurately optimise the cooling system (Castelan *et al.* 2019).

It has been well recognised that an exceptional heat sink can be obtained from simultaneously optimising the heat sink performance and operating cost. The design variables usually consist of fin height, fin diameter, and base plate thickness, however, recent study (Ramphueiphad and Bureerat 2018) reveals that adding fin cross-sections and fin height variation to the set of design variables lead to even better heat sinks. As a result, investigation on the use unconventional design variables for heat sink design is a challenging issue. The use of multi-objective optimisers for geometric and sizing design of heat sinks has been investigated. Therefore, designing such a cooling unit requires optimal geometry to optimise the cooling efficiency (Shi *et al.* 2019). The researchers then developed the design to get the optimum value through various methods such as optimisation of pin fin heat sinks in bypass flow using an entropy generation minimization method (Khan *et al.* 2009). However, growing thermal efficiency in the design of heat transfer generally leads to an increase in the pressure drop across the cooling unit. This requires high pumping energy and consequently has high operating costs. Most scientists, therefore, use the temperature conjunction and fan pumping power as an objective function. In recent years, the use of multiobjective optimisers for geometric and sizing design of microchannel heat sinks has been investigated.

Our past research shows that using MOEAs for the multiobjective design of pin fin and plate fin heat sinks is superior to the classic design approach (Husain and Kim 2010). Other work related to MOEAs and the optimum design of some types of pin fin and plate fin heat sinks can be found in (Jian-hui *et al.* 2009, Kanyakam and Bureerat 2011, Ramphueiphad and Bureerat 2018, Srisomporn and Bureerat 2008, Yang *et al.* 2019). Previous research found that the process of finding the appropriate value takes a long time due to the function evaluation of finite element analysis; therefore performance enhancement of the optimisation of MOEA design is always needed (Ahmed 2016, Hilbert *et al*. 2006, Khan *et al*. 2009, Thiele and Zitzler 1999). The use of a strength Pareto evolutionary algorithm has been studied in combination with a radial-based function and response surface model (RSM) for heat sink platform design (Hadad *et al.* 2019, Husain and Kim 2010, Jian-hui *et al.* 2009, Subasi *et al.* 2016, Thiele and Zitzler 1999, Yang *et al.* 2013). It has been found that the performance of the SPEA is greatly increased with the inclusion of the RBF surrogate model in the evolutionary design process. In the case of pin fin heat sink design, research has been carried out on the use of an integrated Kriging model and PBIL to solve a problem with heat sink design (Husain and Kim 2008, 2010, Thiele and Zitzler 1999). Much of the research in the literature has focused on the optimal fin size, with the fin geometry being constantly predetermined. However, it has been found that better heat sinks can be obtained if fin sizes and other parameters for HS geometries are considered at the same time as the design variables (Haertel *et al.* 2018, Hoi *et al.* 2019, Jian-hui *et al*. 2009).

The main objective of this paper is, therefore, to propose an innovative idea of planting splayed pin fins on a heat sink of a side-inlet-side-outlet type. The new heat sink is termed a Splayed Multiple Cross-Sectional Pin Fin Heat Sink (SMCSPFHS). The design problem has two objective functions: the junction temperature and fan pumping power. Design variables are encoded to shape the heat sink geometry with various fin cross-sections and to be used with multi-objective

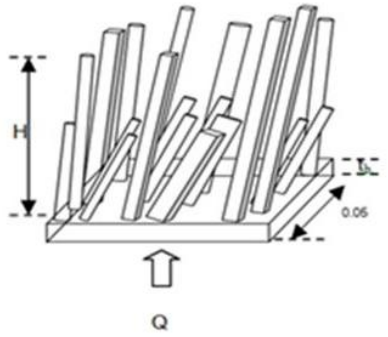

Fig. 1 Side view of splayed multiple cross-sectional pin fin heat sinks

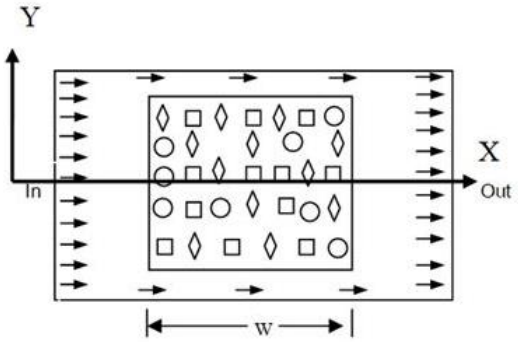

Fig. 2 Top view of splayed multiple cross-sectional pin fin heat sinks

evolutionary algorithms. The results show that the new construction technique gives superior heat sinks to the traditionally used pin fins.

2. Heat sink design

Fig. 1 demonstrates the side views of the splayed multiple cross-sectional pin fin heat sinks (SMCSPFHS). Fig. 2 shows the side-inlet-side-outlet heat sinks and displays the HS top view in cases where pin fins appear to have different cross-sections. The baseplate is $w \times w$, where the width of the heat sink is set as w, the thickness of baseplate set as t_b and the height of the heat sink set as H. The heat load (Q) is constant, and the inlet air velocity V_f cools the heat sink. Fig. 3 details the parameters for defining the angle of splayed multiple cross-sectional pin fin heat sinks (SMCSPFHS) as 30-80 degrees. The fluid domain for this research is 220 mm long, 70 mm high and 57 mm wide.

3. Numerical model

A 3D CFD code is also used to analyse the temperature and flow rates of the heat sink at

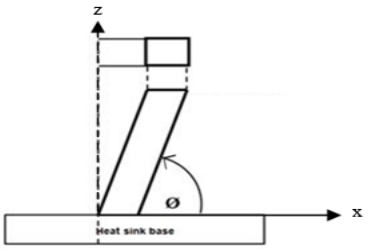

Fig. 3 Schematic of design problems

different air speeds. COMSOL is used to solve the Navier–Stokes equations with the finite-element method for mass, momentum and energy conservation. The turbulent flow model is used for this work because similar conditions have been reported in (Yu *et al.* 2005). that the flow is turbulent in their experimental studies. Radiation heat transfer and boosting effects are insignificant. This simulation assumes the flow as incompressible and steady. It is assumed that the thermodynamic properties are constant. Then the momentum and continuity equations can be written as:

$$\rho(\mathbf{u}\cdot\nabla)\mathbf{u} = \nabla\cdot\left[-p\mathbf{I}+(\mu+\mu_T)(\nabla\mathbf{u}+(\nabla\mathbf{u})^T)-\frac{2}{3}(\mu+\mu_T)(\nabla\cdot\mathbf{u})\mathbf{I}-\frac{2}{3}\rho k\mathbf{I}\right]+\mathbf{F} \tag{1}$$

$$\nabla\cdot(\rho\mathbf{u})=0 \tag{2}$$

The transport equation for k is given by

$$\rho(\mathbf{u}\cdot\nabla)k=\nabla\cdot\left[\left(\mu+\frac{\mu_T}{\sigma_k}\right)\nabla k\right]+P_k-\rho\varepsilon \tag{3}$$

The transport equation for ε is given by

$$\rho(\mathbf{u}\cdot\nabla)\varepsilon=\nabla\cdot\left[\left(\mu+\frac{\mu_T}{\sigma_\varepsilon}\right)\nabla\varepsilon\right]+C_{\varepsilon1}\frac{\varepsilon}{k}P_k-C_{\varepsilon2}\rho\frac{\varepsilon^2}{k} \tag{4}$$

$$\varepsilon=\mathrm{ep} \tag{5}$$

ep = the turbulent dissipation rate

$$\mu_T=\rho C_\mu\frac{k^2}{\varepsilon} \tag{6}$$

$$P_k=\mu_T\left[\nabla\mathbf{u}\colon(\nabla\mathbf{u}+(\nabla\mathbf{u})^T)-\frac{2}{3}(\nabla\cdot\mathbf{u})^2\right]-\frac{2}{3}\rho k\nabla\cdot\mathbf{u} \tag{7}$$

The colon symbol designates matrix contraction.

$$\rho C_\mathrm{p}\mathbf{u}\cdot\nabla T=\nabla\cdot(k_a\nabla T)+\mathrm{Q} \tag{8}$$

The heat equation is

$$\rho_s C_{ps}\frac{\partial T}{\partial t}=\nabla\cdot(k_s\nabla T)+\mathrm{Q} \tag{9}$$

Table 1 Turbulent model (d=0.0035 m, N_f=6, t_b=0.0025 m, V=1 m/s, w=0.05 m)

Mesh sizes (m)	Tetrahedral elements	Junction temperature (K)	Fan pumping power (watt)
0.0011	239,108.00	567.8983	0.048248
0.0012	165,471.00	570.1092	0.050186(4.02%)
0.0013	127,115.00	573.5304	0.052325(8.45%)
0.0014	64,744.00	595.4134	0.053484(10.85%)
0.0015	23,527.00	632.3561	0.057493(19.16%)

The turbulent model parameters are set as (Yu *et al.* 2005)

$$C_{\varepsilon 1} = 1.44, C_{\varepsilon 2} = 1.92, \sigma_\varepsilon = 1.30, \sigma_k = 1.0 \text{ and } C_\mu = 0.09$$

The standard k–ε is used to model the air flow characteristics through the heat sinks. It has been illustrated in the previous study (Ramphueiphad and Bureerat 2018) that using the standard k–ε model gives good prediction of heatsink performance indicators compared to the experiment results. k and ε were specified at the inlet, and zero gradients were assumed in the z direction at the outlet. The heat generated by unit area is Q; the temperature in the heat sink is the temperature variable T and the thermal conductivity variable k_s. The velocity of air flow, on the walls, non-slip boundary conditions were provided for speed. The standard wall functions have been used to treat the surrounding wall area. A uniform heat flux on the lower surface of the fin base was applied.

The COMSOL CFD software was used to model the heat transfer and fluid phenomena for configuring the heatsinks. The COMSOL CFD kit was chosen because the pre-processor (geometry and mesh generation) and the solver are integrated. COMSOL Multiphysics Finite Element Analysis (FEA) software has been used to develop CFD models for heatsinks; and to investigate the predictive accuracy of junction temperature and fan pumping power predictions using k- ε turbulence models. Uses Reynolds Average Navier-Stokes (RANS) models which divide the flow amount into an average value and fluctuate the component. When the flow has turned chaotic, all amounts fluctuate in space and time. Detailed information on the fluctuations is extremely computationally costly. An average depiction often provides enough information about the flow. COMSOL used conjugate heat transfer.

3.1 Mesh dependency and validation

Finite volume analysis (FVA) with finite element analysis was used to validate the experiment to ensure a credible evaluation of the pressure drop and the heat transfer function in a heat sink (Yu *et al.* 2005). Data on the heat sink was reported finite elements analysis (FEA) and FVA errors were less than 10%. This design heat sink used FEA. The Finite Element Analysis (FEA) is used to solve the above-mentioned regulatory equations.

A 3D tetrahedral mesh form with 4 corner points appropriate for the geometry of the domain and numerical diffusion is selected. Default values provided by the COMSOL software are used. For mesh consistency checking we use mesh sizes of 0.0011 m, 0.0012 m, 0.0013 m, 0.0014 m and 0.0015 m. Table 1 compares the effects of different mesh sizes on the expected junction temperature and fan pumping capacity. The bracket values are the percentage of temperature errors and pumping power in relation to the value of 0.0011 m mesh. For a mesh size of 0.0011 m, the optimization procedure is expected to be much more accurate but time-consuming, whereas the

objective functions (junction temperature and fan pump power) obtained are significantly different from the results achieved using the 0.0012 m mesh for relative percent errors of 0.39% and 4.02 percent, respectively. The mesh size of 0.0012 m is therefore used in this analysis to reduce run time for optimisation.

4. Optimisation method

4.1 Objective function

The air flow was adjusted to be side- inlet-side-outlet. HS air impingement can cause back pressure on the electrical system; however, this heat sink has some significant advantages because back pressure is not caused. Aluminium was used as a heat sink, with a much higher thermal conductivity=202 W/m K, a specific heat=871 J/kg K and a density=2719 kg/m^3, but it is mechanically soft. The air properties were density=1.177 kg/m^3, specific heat=1006 J/kg K, thermal conductivity=0.0267 W/m K and viscosity=1.8832 $\times$ 10^{-5} kg/m s. The base dimensions were 50 mm $\times$ 50 mm. The pin fins were to be planted with different fin heights, distribution and cross-sections. The following defines the multi-objective design problem

$$\text{Min: } \mathbf{f} = \{f_1(\mathbf{x}), f_2(\mathbf{x})\} \tag{10}$$

subject to

$$T_j - 360 \text{ K} \leq 0$$
$$\mathbf{x}_L \leq \mathbf{x} \leq \mathbf{x}_U$$

When the junction temperature was $f_1(\mathbf{x})$ or (T_j) between the plate base and the electronic equipment, the fan pumping power (P_f) was $f_2(\mathbf{x})$. The highest operating temperature is the connection temperature between the base plate and the electronic equipment. The heat sink is used to prevent the junction temperature not exceeding 360 K, the limited temperature that causes the CPU being less efficient. The pumping power is the power required to operate the ventilator at the speed of the inlet air. It is possible to express both objective functions as

$$f_1(\mathbf{x}) = T_j = T_a + QR_{HS}(\mathbf{x}) \tag{11}$$

and

$$f_2(\mathbf{x}) = P_f = \frac{\dot{m}(\mathbf{x})\Delta P(\mathbf{x})}{\rho_a} \tag{12}$$

The variable T_a is the ambient air temperature at the inlet, set to 298 K, Q is the heat load on the bottom base heat sinks and is set to 22,000 W /m^2, R_{HS} is the thermal resistance of the heat sink (K/m^2), $\dot{m}$ is the flow rate of air (kg/s), ρ is the density of air (kg/m^3) and ΔP is the pressure drop across the splayed pin fin heat sink (N/m^2). CFD software was used in this work to calculate the pressure and temperature values.

4.2 Encoding / decoding

The heat sink is programmed to remain symmetrical to the xz plane. The fin number, base thickness and air inlet velocity, cross-sectional fins, fin diameters and fin heights are defined as the design variables. Fig. 5 provides an example of such thermal sink with the coded fins. The number

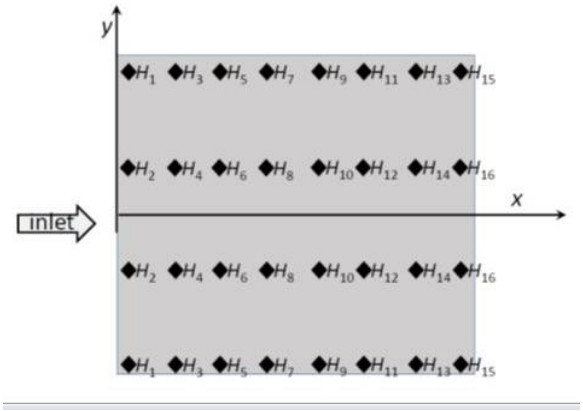

Fig. 4 Control points for the distribution of fin height

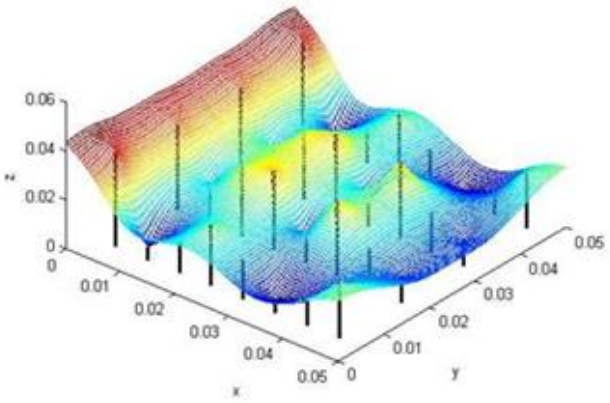

Fig. 5 RBF surface to maintain control of the distribution of fin height

of such design variables in the x direction is 3 $n_{x,max}$ +19 rows and the upper limit of the number of such rows is set to $n_{x,max}$ in the x direction. The vector **x** design decoding process (Algorithm 1) shows a heat sink model. The base of the fin is a square plate set to *w* and t_b is the plate thickness. The number of fin rows (n_x) in the x direction is then assigned as *ceil*(x_1), where *ceil*(x) indicates the ceiling of ***x*** (n_x=8 in Fig. 4), and x_2 and x_3 are the base thickness and air velocity of the inlet. The next $n_{x,max}$ elements of **x** are assigned to the number of fins on $n_{x,max}$ rows along the x direction and are saved to the n vector, the lower and upper limits of which are $n_{x,min}$ and $n_{x,max}$. The round function gives its input value to the nearest integer, in Fig. 4, for example. n {4, 6, 5, 7, 6, 6, 6, and 4} is the first 8 elements. There are three cross-sections for this work, a circle, a diamond and a square. The fins are arranged in each row so that the xz plane is symmetrical. The following $n_{x,max}$ elements are then assigned to vectors for specifying the cross-section types. The lower and upper boundaries of **s** are 1 and 3 with the square cross-section 1 respectively, the diamond cross-section 2 and the circular cross-section 3. In Fig. 4, the **s** value is {1, 3, 3, 2, 1, 2, 1}. The following $n_{x,max}$ elements of **x** are assigned to **d,** a vector with a fin diameter for each row of fins. Note that n_x values only in **n**, **s**, and **d** are used to generate a heat sink. However, for these vectors, $3n_{x,max}$ elements of x must be saved if the decoding value of n_x is equal to $n_{x,max}$. The position of the

Algorithm 1 Decoding of design variables

Heat Sink Geometry
Input defined parameters nx,min, nx,max, ny,min, ny,max, W; design variables x sized ($3_{nx,max}$+19) x 1
Output Heat sinks dimensions and geometry
1. Parameters are set
$nx = ceil(x_1)$, $t_b = x_2$, $V_f = x_3$, $\emptyset = x_4$
n = *round*(xi), for $i = 4, \ldots, n_{x,max}+3$
s = *round*(xi), for i = $n_{x,max}+4, \ldots, 2_{nx,max}+3$
d = x_i, for $i = 2n_{x,max} + 4, \ldots, 3n_{x,max} + 3$
H = x_i, for $i = 3n_{x,max} + 4, \ldots, 3n_{x,max} + 19$
2. To calculate the fin height distribution, also in accordance with Fig. 4, create 8 x 4 co ntrol points.
3. Designate the values of 16 H elements to control points just after Fig. 4.
4. The RBF interpolation model is used to create the distribution of fin height.
5. Stipulate the number of fins from each row set as ni, for $i = 1, \ldots, n_x$.
6. Specify a cross-section type for each row set as si, for $i = 1, \ldots, n_x$.
7. Determine the size of the fin in each row set as di, for $i = 1, \ldots, n_x$.
8. The fins (xi, y_i) are created on the basis of the fin using steps 5-7 as well.
9. Use the RBF predictor to evaluate the fin height per each point (Ghale *et al*. 2015).
10. Export all data to the CFD software

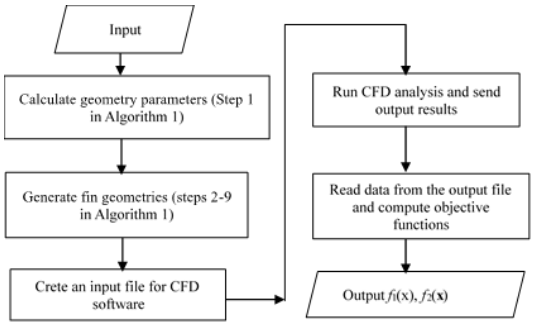

Fig. 6 Flowchart for function evaluation of splayed pin fin heat sink optimal design

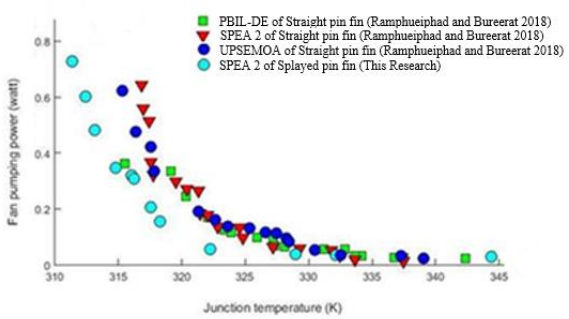

Fig. 7 Pareto fronts comparison of various design results

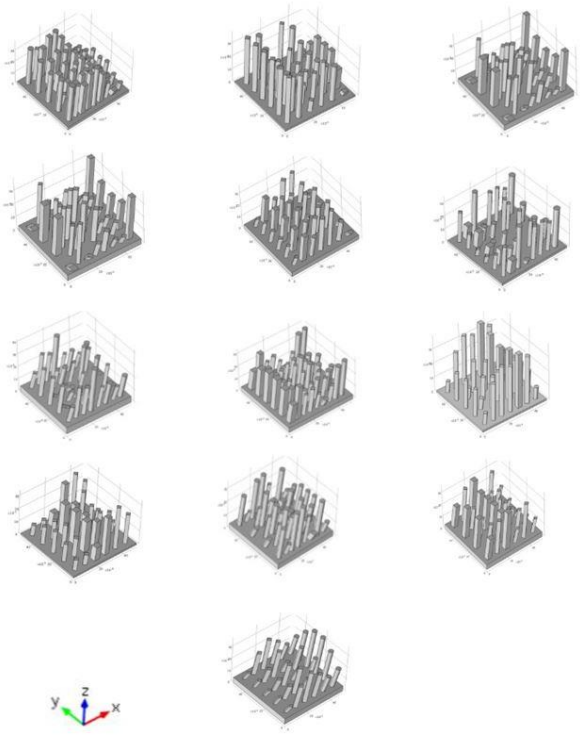

Fig. 8 Selected heat sink geometries from Pareto optimal solutions

fins can be specified on the base plate with all the above data types. The fin height is then calculated to obtain a symmetrical heat sink. In this work, 16 elements of x with the $[H_{min}, H_{max}]$ lower and upper boundaries are assigned to the vector $\mathbf{H_0}$, which is used to control the height distribution of the fin. The elements of $\mathbf{H_0}$ are distributed in the Fig. 4. In both the x and y directions the control points are equally spaced at N= 4 × 8. Because the control points set as X_0 and Y_0 are the vectors with the x and y coordinates, the RBF interpolation is used to calculate the fin height at a certain point (x, y).

$$H(x,y) = \sum_{i=1}^{N} c_i K\left(\sqrt{\left(x - x_{0,i}\right)^2 + \left(y - y_{0,i}\right)^2}\right) \tag{13}$$

Where $K(r)$ is a kernel function that in this work is set to a linear spline $K(r)=r$. $(x_{0,i}, y_{0,i})$ is the i-th control point coordinate. The coefficients c_i are computed to solve the linear equations system.

$$H\left(x_{0,j}, y_{0,j}\right) = \sum_{i=1}^{N} c_i K(r_{ij}) \quad \text{for } j = 1, \ldots, N. \tag{14}$$

The r_{ij} variable is the distance between the i-th and j-th control points. $H(x_0,j, y_0,j)$ is the $\mathbf{H}_0$ element assigned to the j-th control point (Fig. 4). Fig. 5 displays a specific RBF response surface calculated from a specific $\mathbf{H}_0$, where the resulting fin height distribution and the different cross-sections of the fins are shown in Fig. 4. The optimisation process is shown in Fig. 6. This work uses MATLAB to create a COMSOL input file. In the batch mode in which output results are sent,

CFD analysis is performed. The results are read and calculated by MATLAB as objective function values.

5. Results and discussions

Fig. 7 displays the results from various design strategies. Those include the Pareto fronts obtained from splayed pin fin design using SPEA2, straight pin fin design using hybrid population-based incremental learning and differential evolution (PBIL-DE), straight pin fin design using SPEA2, and straight pin fin design using an unrestricted population size evolutionary multiobjective optimization algorithm (UPSEMOA). It is seen that the results from the splayed pin fin design using SPEA2 proposed in this paper totally dominate the other Pareto fronts. The front of the splayed pin fin heat sink is far superior to those of the straight pin fin design particularly for the junction temperature, which is a thermal performance indicator. This implies that the proposed splayed pin fin heat sink design in this paper leads to higher performance heat sinks. Fig. 8 displays thirteen heat sinks from the Pareto front of the splayed pin fin design (light blue circle markers in Fig. 7). The heat sinks are shown beginning from the one that provides the minimum fan pumping power to the one that provides the minimum junction temperature. The heat sinks have distinct geometries, with various fin height distribution, fin orientations, and fin cross-sections. Validation of the new heat sinks with those heat sinks used in reality can be made by comparing to the results presented in (Ramphueiphad and Bureerat 2018) where conventional pin fin and plate fin heat sinks from (Yu *et al*. 2005) with the side-inlet-side-outlet conditions are analysed with several inlet air velocities ranging from 1 m/s to 6 m/s. The comparative results shown in the reference that those conventional heat sinks where totally dominated by the straight pin fin design fronts in Fig. 7. That means the splayed pin fin deign front will also dominates the conventional heat sinks. The hypervolume values of the fronts plotted in Fig. 7 are calculated where the reference point is set at f_1=392.46 K and f_2=1.0189 Watt. The greater hypervolume means the better front. The front hypervolumes of straight pin fin design obtained from PBIL-DE, UPSEMOA and SPEA2 are respectively 72.484, 75.8222 and 66.0137. On the other hand, the front hypervolume of splayed pin fin obtained from SPEA2 is 188.2386. This implies the splayed pin fin design is far superior to the straight pin fin design.

6. Conclusions

This study uses the second version of a strength Pareto evolutionary algorithm (SPEA2) to address the new problem of multi-objective optimisation design of splayed multiple cross-sectional pin fin heat sinks (SMCSPFHS). Objective functions are the fan pumping power and junction temperature. Function evaluations can be accomplished using computational fluid dynamics (CFD) analysis. Design variables include pin cross-sectional areas, the number of fins, fin pitch, thickness of heat sink base, inlet air speed, fin heights, and fin orientations with respect to the base. Design constraints are defined in such a way as to make a heat sink usable and easy to manufacture. Compared the result with the straight cross-section pin heat sinks with the optimisers as: PBIL-DE, SPEA2, and UPSEMOA, the sprayed pin fin design is superior to those results from the straight pin fin cases. For future work, investigation on the use of surrogate modelling for the splayed pin fin design will be conducted. This should lead to a more efficient design process for the splayed pin fin heat sinks.

Acknowledgments

This research was supported by the Sustainable and Infrastructure Research and Development Center and Rajamangala University of Technology Isan, Nakhonrachisima and the ThailandResearch Fund (TRF).

References

Ahmed, H.E. (2016), "Optimization of thermal design of ribbed flat-plate fin heat sink", *Appl. Therm. Eng.*, **102**, 1422-1432. https://doi.org/10.1016/j.applthermaleng.2016.03.119.

Bahiraei, M. and Heshmatian, S. (2017), "Optimizing energy efficiency of a specific liquid block operated with nano fluids for utilization in electronics cooling : A decision-making based approach", *Energ. Convers. Manag.,* **154**,180-190. https://doi.org/10.1016/j.enconman.2017.10.055.

Bahiraei, M., Heshmatian, S. and Keshavarzi, M. (2018), "Multi-attribute optimization of a novel micro liquid block working with green graphene nano fl uid regarding preferences of decision maker", *Appl. Therm. Eng*., **143**, 11-21. https://doi.org/10.1016/j.applthermaleng.2018.07.074.

Bahiraei, M., Heshmatian, S. and Keshavarzi, M. (2019), "A decision-making based method to optimize energy efficiency of ecofriendly nanofluid flow inside a new heat sink enhanced with flow distributo*r*", *Powder. Tech.*, **342**, 85-98. https://doi.org/10.1016/ j.powtec.2018.10.007.

Bahiraei, M., Heshmatian, S. and Keshavarzi, M. (2019), "Multi-criterion optimization of thermohydraulic performance of a mini pin fin heat sink operated with ecofriendly graphene nanoplatelets nanofluid considering geometrical characteristics", *J. Mol. Liq.*, **276**, 653-666. https://doi.org/10.1016/ j.molliq.2018.12.025.

Castelan, A., Cougo, B., Dutour, S. and Meynard, T. (2019), "3D analytical modelling of plate fin heat sink on forced convection", *Math. Comput. Simul.*, **158**, 296-307. https://doi.org/10.1016/j.matcom.2018.09.011.

Hadad, Y., Ramakrishnan, B., Pejman, R., Rangarajan, S., Chiarot, P.R., Pattamatta, A. and Sammakia, B. (2019), "Three-objective shape optimization and parametric study of a micro-channel heat sink with discrete non-uniform heat flux boundary conditions", *Appl. Therm. Eng.*, **150**(January), 720-737. https://doi.org/10.1016/j.applthermaleng.2018.12.128.

Haertel, J.H.K., Engelbrecht, K., Lazarov, B.S. and Sigmund, O. (2018), "Topology optimization of a pseudo 3D thermofluid heat sink model", *Int. J. Heat Mass Transf.*, **121**, 1073-1088. https://doi.org/10.1016/j.ijheatmasstransfer.2018.01.078.

Hilbert, R., Janiga, G., Baron, R. and Thévenin, D. (2006), "Multi-objective shape optimization of a heat exchanger using parallel genetic algorithms", *Int. J. Heat Mass Transf.*, **49**(15-16), 2567-2577. https://doi.org/10.1016/j.ijheatmasstransfer.2005.12.015.

Hoi, S.M., Teh, A.L., Ooi, E.H., Chew, I.M.L. and Foo, J.J. (2019), "Plate-fin heat sink forced convective heat transfer augmentation with a fractal insert", *Int. J. Therm. Sci.*, **142**(April), 392-406. https://doi.org/10.1016/j.ijthermalsci.2019.04.035.

Husain, A. and Kim, K.Y. (2008), "Optimization of a microchannel heat sink with temperature dependent fluid properties", *Appl. Therm. Eng.*, **28**(8-9), 1101-1107. https://doi.org/10.1016/j.applthermaleng.2007.12.001.

Husain, A. and Kim, K.Y. (2010), "Enhanced multi-objective optimization of a microchannel heat sink through evolutionary algorithm coupled with multiple surrogate models", *Appl. Therm. Eng.*, **30**(13), 1683-1691. https://doi.org/10.1016/j.applthermaleng.2010.03.027.

Jian-hui, Z., Chun-Xin, Y. and Li-na, Z. (2009), "Minimizing the entropy generation rate of the plate-finned heat sinks using computational fluid dynamics and combined optimization", *Appl. Therm. Eng.*, **29**(8-9), 1872-1879. https://doi.org/10.1016/j.applthermaleng.2008.08.001.

Kanyakam, S. and Bureerat, S. (2011), "Multiobjective evolutionary optimization of splayed pin-fin heat

sink", *Eng. Appl. Comput. Fluid Mech.*, **5**(4), 553-565. https://doi.org/10.1080/19942060.2011.11015394.
Khan, W.A., Culham, J.R. and Yovanovich, M.M. (2009), "Optimization of microchannel heat sinks using entropy generation minimization method", *IEEE Trans. Components Packag. Technol.*, **32**(2), 243-251. https://doi.org/10.1109/TCAPT.2009.2022586.
Ramphueiphad, S. and Bureerat, S. (2018), "Synthesis of multiple cross-section pin fin heat sinks using multiobjective evolutionary algorithms", *Int. J. Heat Mass Transf.*, **118,** 462-470. https://doi.org/10.1016/j.ijheatmasstransfer.2017.11.016.
Shi, X., Li, S., Mu, Y. and Yin, B. (2019), "Geometry parameters optimization for a microchannel heat sink with secondary flow channel", *Int. Commun. Heat Mass Transf.*, Elsevier, **104**(March), 89-100. https://doi.org/10.1016/j.icheatmasstransfer.2019.03.009.
Srisomporn, S. and Bureerat, S. (2008), "Geometrical design of plate-fin heat sinks using hybridization of MOEA and RSM", *IEEE Trans. Components Packag. Technol.*, **31**(2 SPEC. ISS.), 351-360. https://doi.org/10.1109/TCAPT.2008.916799.
Subasi, A., Sahin, B. and Kaymaz, I. (2016), "Multi-objective optimization of a honeycomb heat sink using Response Surface Method", *Int. J. Heat Mass Transf.*, **101**, 295-302. https://doi.org/10.1016/j.ijheatmasstransfer.2016.05.012.
Thiele, L. and Zitzler, E. (1999), "Multiobjective evolutionary algorithms: A comparative case study and the strength pareto approach", *IEEE Trans. Evol. Comput.*, **3**(4), 257-271.
Yang, A., Chen, L., Xie, Z., Feng, H. and Sun, F. (2019), "Constructal operation cost minimization for in-line cylindrical pin-fin heat sinks", *Int. J. Heat Mass Transf.*, **129**, 562-568. https://doi.org/10.1016/j.ijheatmasstransfer.2018.09.129.
Yang, Y.T., Lin, S.C., Wang, Y.H. and Hsu, J.C. (2013), "Numerical simulation and optimization of impingement cooling for rotating and stationary pin-fin heat sinks", *Int. J. Heat Fluid Flow*, **44**, 383-393. https://doi.org/10.1016/j.ijheatfluidflow.2013.07.008.
Yu, X., Feng, J., Feng, Q. and Wang, Q. (2005), "Development of a plate-pin fin heat sink and its performance comparisons with a plate fin heat sink", *Appl. Therm. Eng.*, **25**(2-3), 173-182. https://doi.org/10.1016/j.applthermaleng.2004.06.016.

WT